THE JOURNAL OF PHYSICAL CHEMISTRY A
A JOURNAL OF THE AMERICAN CHEMICAL SOCIETY

pubs.acs.org/JPCA

Article

Binding Strengths and Orientations in CO_2 Adsorption on Cationic Scandium Oxides: Governing Factor Revealed by a Combined Infrared Spectroscopy and Theoretical Study

Pengcheng Liu, Jia Han,* Yan Chen, Haili Yu, Xiaoguo Zhou,* and Weijun Zhang*

Cite This: *J. Phys. Chem. A* 2024, 128, 3007−3014

Read Online

ACCESS | Metrics & More | Article Recommendations | Supporting Information

ABSTRACT: Carbon dioxide (CO_2) adsorption is a critical step to curbing carbon emissions from fossil fuel combustion. Among various options, transition metal oxides have received extensive attention as promising CO_2 adsorbents due to their affordability and sustainability for large-scale use. Here, the nature of binding interactions between CO_2 molecules and cationic scandium oxides of different sizes, i.e., ScO^+, $Sc_2O_2^+$, and $Sc_3O_4^+$, is investigated by mass-selective infrared photodissociation spectroscopy combined with quantum chemical calculations. The well-accepted electrostatic considerations failed to provide explanations for the trend in the binding strengths and variations in the binding orientations between CO_2 and metal sites of cationic scandium oxides. The importance of orbital interactions in the driving forces for CO_2 adsorption on cationic scandium oxides was revealed by energy decomposition analyses. A molecular surface property, known as the local electron attachment energy, is introduced to elucidate the binding affinity and orientation-specific reactivity of cationic scandium oxides upon the CO_2 attachment. This study not only reveals the governing factor in the binding behaviors of CO_2 adsorption on cationic scandium oxides but also serves as an archetype for predicting and rationalizing favorable binding sites and orientations in extended surface−adsorbate systems.

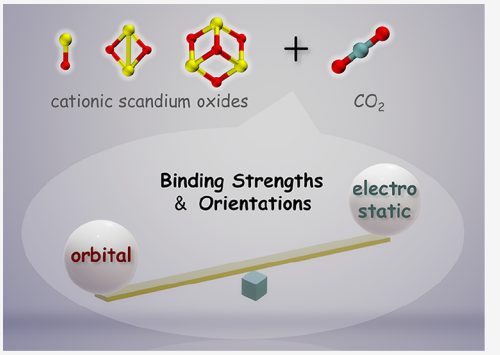

1. INTRODUCTION

The ever-rising level of carbon dioxide (CO_2) in the atmosphere and resulting global warming have become one of the most pressing environmental concerns of our age. CO_2 capture and sequestration (CCS) and CO_2 capture and utilization (CCU) hold great promise not only for mitigating anthropogenic greenhouse gas emissions but also for providing a bridging strategy to achieve carbon-free energy systems.[1,2] Recent years have witnessed the rapid development of energy-efficient, cost-effective, and sustainable materials for CO_2 capture and subsequent sequestration or utilization. In the past decades, both liquid and solid-phase CO_2 capturing materials have been reported for their potential implementations in effective reduction of CO_2 emissions, among which transition metal oxides have received increasing attention due to high adsorption performance and low regeneration energy consumption.[3−6] Hence, it is of great scientific importance to develop a comprehensive understanding of the nature of binding interactions in adsorption processes between transition metal oxide adsorbents and CO_2 molecules, aiming to facilitate the rational design and improvement of transition metal oxide materials with a high CO_2 adsorption capacity.

In many cases, active centers that are responsible for the CO_2 uptake usually amount to the uppermost atomic layers on the surface of sorbent materials.[7] However, one of the stumbling blocks in the way is the complexity of the "real" surface conditions that impairs the efforts to unravel the underlying adsorption mechanisms. Gas-phase studies on metal ion−molecules complexes in an unperturbed environment can serve as an ideal approach to reveal the intrinsic interactions between active components at the molecular level.[8,9] Experimental and theoretical investigations have been carried out to explore the adsorption behaviors of CO_2 molecules on transition metal oxides under different charge states. Chemisorption of CO_2 with the formation of carbonate or oxalate structures was normally identified for negatively charged transition metal oxides due to efficient charge transfer processes.[10−12] On the other hand, both physisorption and chemisorption were predicted to be thermodynamically feasible for neutral transition metal oxides, where the preference for specific binding motifs depends on the composition and size of the corresponding clusters.[13−15] In the studies of cationic transition metal oxides, weakly

Received: March 10, 2024
Revised: March 22, 2024
Accepted: March 25, 2024
Published: April 6, 2024

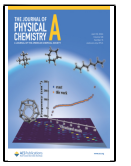

https://doi.org/10.1021/acs.jpca.4c01562
J. Phys. Chem. A 2024, 128, 3007−3014

physisorbed CO_2 with a linear geometry was found to be the dominant adsorption mode at small complex sizes, while the conversion from molecularly bound forms to carbonate-containing structures occurs upon successive addition of CO_2 molecules.[16−20] The general trend of CO_2 molecule adsorption onto positively charged metal oxides is relatively straightforward, which is, however, more practical in the CCS and CCU applications from the perspective of long-term regenerability.

Among the transition metal oxides employed in capturing and conversion processes, scandium oxides have proven to be valuable materials due to their potential applications in heterogeneous reactions as efficient promoters and supports.[21−25] Structures and interactions of small cationic scandium oxides (e.g., ScO^+ and $Sc_2O_2^+$) with CO, CO_2, and H_2O molecules have been experimentally and theoretically investigated, providing crucial information on elementary reaction processes.[18,20,26−28] However, fundamental studies on cationic scandium oxides at medium and large sizes remain scarce,[29,30] in which of particular interest is the Sc_3O_4 structure that has been determined to be the surface termination in Sc-enriched bulk materials.[31] The gas-phase reactions of the $Sc_3O_4^+$ cation with CO_2 molecules can serve as a well-defined model system for the adsorption of CO_2 to cluster-like active centers on Sc-based adsorbent surfaces. Furthermore, a systematic examination of the interactions between the CO_2 molecule and cationic scandium oxides of varying sizes allows for uncovering the mechanistic details in the CO_2 adsorption behaviors on scandium oxides.

In the current study, we first perform infrared photodissociation spectroscopy combined with density functional theory (DFT) calculations on the ion−molecule complex composed of the $Sc_3O_4^+$ cation and the CO_2 molecule, in order to provide insights into the binding motifs and crucial intermolecular interactions. After structural characterization for the $[Sc_3O_4(CO_2)]^+$ complex ion, the trend in binding interactions between CO_2 and cationic scandium oxides of difference sizes, i.e., ScO^+, $Sc_2O_2^+$, and $Sc_3O_4^+$, is thoroughly investigated, aiming to elucidate binding mechanisms and reactivity patterns of cationic scandium oxides toward CO_2 adsorption at the molecular level.

2. METHODS

2.1. Experimental Methods. The infrared photodissociation spectrum of $[Sc_3O_4(CO_2)]^+$ complex ion was measured using a collinear tandem time-of-flight (TOF) mass spectrometer equipped with a laser vaporization ion source as described previously.[20] In brief, a Nd:YAG laser operating at 532 nm was used to vaporize the simultaneously rotating and translating scandium metal target. The ion−molecule complexes were generated by the reactions of the vaporized species with CO_2 molecules in the presence of helium carrier gas seeded with 10% CO_2. Backing pressure of the reaction gas was adjusted in the range of 4.0−6.0 × 10^5 Pa to obtain desired ion intensities and size distributions. After free expansion, the ions of interest were mass-selected, decelerated into the extraction region of a second-stage TOF mass spectrometer, and then intersected by a tunable IR laser. Typical infrared photodissociation spectra were recorded by monitoring the fragment ions as a function of the IR photon energy and normalized to the parent ion signal and IR laser energy. Tunable IR radiation was scanned in steps of 2 cm^{-1} while narrowing down to 1 cm^{-1} from 2250 to 2450 cm^{-1} for extracting detailed spectral substructures.

2.2. Theoretical Methods. Quantum chemical calculations were performed to identify energetically lowest-lying structures of target ion−molecule complexes. Genmer[32,33] was used to extensively and randomly generate initial guess structures of the studied species. The semiempirical quantum mechanical method GFN2−xTB[34] was employed to preoptimize complex geometries using the xtb[35] program. Further geometry optimization was performed using density functional theory (DFT) at the PBE0−D3(BJ)/def2−TZVP level of theory.[36,37] Vibrational frequency analyses at the same density functional level were conducted to ensure that all found minima have zero imaginary frequency and to compute zero-point energies (ZPEs). All the DFT calculations were performed with the Gaussian 16 software package.[38] More accurate single point energies were computed at the CCSD(T)/def2-TZVPP level of theory using the ORCA suite of program.[39,40] Simulated IR spectra were derived from the calculated harmonic vibrational frequencies scaled by a factor of 0.957 and further convoluted with Lorentzian functions using 15 cm^{-1} full width at half-maximum (fwhm) to reproduce spectral features. The scaling factor was determined by comparing the experimental and calculated values of the antisymmetric stretching vibrational frequency of free CO_2 molecule. Energy decomposition analysis (EDA) was conducted using the sobEDA method based on Gaussian 16 and the Multiwfn program.[32,41]

3. RESULTS AND DISCUSSION

The target cationic ion−molecule complex, $[Sc_3O_4(CO_2)]^+$, is prepared by the pulsed laser vaporization of a scandium metal target in the expansion of helium seeded with CO_2. Figure S1 provides the resulting mass spectrum dominated by the $Sc_3O_4^+$ cation, indicating a large population and high thermodynamic stability of this core structure. Consistent with previous studies,[42,43] the most stable isomer of $Sc_3O_4^+$ cation is predicted to be a cage-like structure with C_{3v} symmetry as shown in Figure S2, where a central O atom triply coordinates to three Sc atoms. This structure was taken as a starting point in the subsequent computational search for possible candidates for the $[Sc_3O_4(CO_2)]^+$ ion−molecule complex. Similar to the findings in our previous report on $Sc_2O_2^+$ cation complexed with CO_2 molecules,[20] both end-on and carbonate-containing configurations were theoretically identified for the $[Sc_3O_4(CO_2)]^+$ complex ion with small energy differences (Figure S3). The corresponding infrared photodissociation spectrum was obtained via monitoring of the CO_2 loss upon tunable IR laser irradiation in the spectral range related to CO_2 antisymmetric stretching vibrations. Carbonate-containing structures are therefore not taken into consideration due to the lack of absorptions in the relevant frequency range, albeit with lower energies. For the molecularly bound form, only one isomer has been identified, given the three equivalent Sc binding sites on the $Sc_3O_4^+$ cation.

Figure 1 shows the mass-selected experimental spectrum recorded in the region of 2100−2500 cm^{-1}, which consists of two partially resolved peaks at 2355 and 2369 cm^{-1}, respectively. By comparison with the simulated IR spectrum of the end-on isomer, the feature at 2369 cm^{-1} at the higher energy side is attributed to the antisymmetric stretching mode of CO_2 in the end-on isomer predicted at 2381 cm^{-1}. The red shift in the experimental spectrum with respect to the theoretical value may arise from the anharmonicity effect, which is commonly involved in multiphoton absorption

https://doi.org/10.1021/acs.jpca.4c01562
J. Phys. Chem. A 2024, 128, 3007−3014

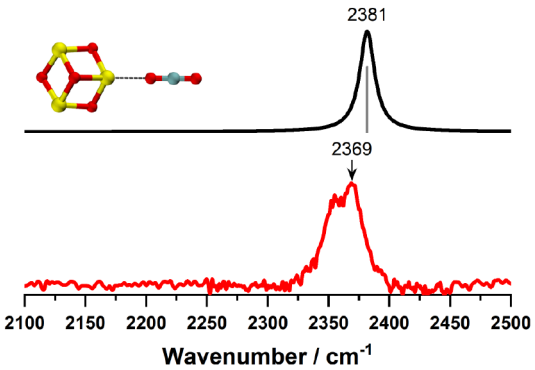

Figure 1. Experimental infrared photodissociation spectrum of $[Sc_3O_4(CO_2)]^+$ complex ion in the spectral range of 2100−2500 cm^{-1} together with the simulated IR spectrum of the end-on isomer obtained at the PBE0-D3(BJ)/def2-TZVP level of theory.

processes that are required to detach the CO_2 ligand. Moreover, note that the CO_2 antisymmetric stretching of this isomeric structure is insufficient to further explain the lower-frequency band centered at 2355 cm^{-1}. Such a small blue shift of 6 cm^{-1} relative to the antisymmetric stretching vibrational frequency of free CO_2 (2349 cm^{-1}) indicates a considerably weaker interaction between attached CO_2 and the metal atom. Theoretically, this band can be interpreted as a combination band of various oscillators in this end-on isomer, or it may originate from the anharmonic coupling of a fundamental mode and overtones in a Fermi resonance. In addition, the presence and dissociation of an energetically high-lying isomer may contribute to this (a tentative assignment is included in the Supporting Information). However, it is hard to draw an unambiguous conclusion here due to the limited spectral resolution.

It is well-accepted that the weak interaction between positively charged metal atoms and CO_2 molecules in the aforementioned end-on binding motifs is dominated by the charge-quadrupole interaction with an electrostatic nature.[44−47] Therefore, in transition metal oxides with a significant ionic component in the M−O bond, the higher atomic charge placed on the metal atom is accordingly expected to bind CO_2 molecule more strongly.[48] To validate the hypothesis of the correlation between the atomic charge distribution and binding strength, the binding energies between the CO_2 molecule and different cationic scandium oxides, i.e., ScO^+, $Sc_2O_2^+$, and $Sc_3O_4^+$, along with the calculated natural population analysis (NPA) atomic charges on Sc atoms are compared in Figure 2. A decreasing trend in binding energies between CO_2 and cationic scandium oxides was observed along the series ScO^+ > $Sc_2O_2^+$ > $Sc_3O_4^+$, in agreement with the pattern of increasing bonding lengths. The situation that CO_2 molecule binds to $Sc_2O_2^+$ cation more strongly than to $Sc_3O_4^+$ is also demonstrated by the greater blue-shift in the CO_2 antisymmetric vibrational frequency of 2376 cm^{-1} observed for $[Sc_2O_2(CO_2)]^+$ complex ion[20] compared to the measurement in this work for $[Sc_3O_4(CO_2)]^+$ (2369 cm^{-1}). The Sc atom of ScO^+ cation carries the highest positive charge of 1.81e, reflecting the significant ionic character $Sc^{2+}O^-$ of the bare ScO^+ cation,[28] and exhibits the strongest ability to terminally bind CO_2 molecule. For the $Sc_2O_2^+$ cation with C_{2v} symmetry,[20] the atomic charges positioned on two Sc atoms are calculated to be 1.67e and 1.46e, respectively. The optimization for CO_2

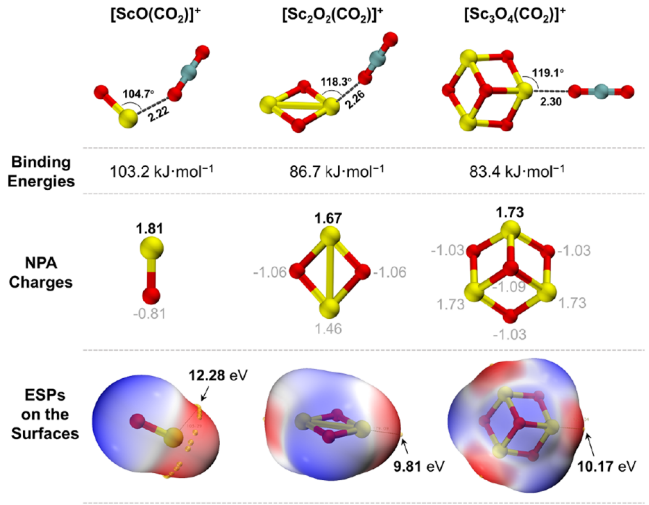

Figure 2. Low-lying structures of the $[ScO(CO_2)]^+$, $[Sc_2O_2(CO_2)]^+$, and $[Sc_3O_4(CO_2)]^+$ ion−molecule complexes in end-on binding motifs calculated at the PBE0-D3(BJ)/def2-TZVP level of theory, together with the binding energies between cationic scandium metal oxides and the CO_2 molecule obtained using the zero-point corrected energies at the CCSD(T)/def2-TZVPP // PBE0-D3(BJ)/def2-TZVP level. Bond lengths are noted in Å. (Top panel) Atomic charges of the ScO^+, $Sc_2O_2^+$, and $Sc_3O_4^+$ cations derived from natural population analysis (NPA) at the PBE0-D3(BJ)/def2-TZVP level of theory. (Middle panel) Electrostatic potential on the molecular surfaces of the ScO^+, $Sc_2O_2^+$, and $Sc_3O_4^+$ cations, computed on the 0.001 e/bohr^3 contour of electron density. Yellow dots indicate the location of the corresponding local maxima on the surfaces. Red regions indicate electron-deficient positive molecular electrostatic potentials, while blue regions correspond to less positive electrostatic potentials (Bottom panel).

initially adhering to the less positively charged Sc atom converged to essentially the same configuration where CO_2 attaches to the Sc atom with a higher net charge. The three Sc atoms of $Sc_3O_4^+$ cation possess identical positive charges of 1.73e, greater than the corresponding value in $Sc_2O_2^+$ cation, and are expected to bind the CO_2 molecule more tightly. However, it turns out that this is not the case, as the binding energy between $Sc_3O_4^+$ cation and the CO_2 molecule is 3.3 kJ·mol^{-1} lower than the analogue calculated for $Sc_2O_2^+$ cation. In other words, there is no direct correspondence between the atomic charges residing on the Sc atoms and their binding affinities toward the CO_2 molecule.

In dealing with noncovalent interactions that are primarily electrostatic in nature, it is more reasonable to quantitively examine electrostatic potentials on the three-dimensional molecular surface, V_S, as it is by way of these, reactant molecules or ions are able to "see" and "perceive" the approaching species.[49−51] Surface areas of positive electrostatic potentials can promote nucleophilic interactions, whereas negative regions favor electrophilic attacks. In cationic scandium oxide systems, positive electrostatic potentials prevail over the entire molecular surface due to the overwhelming effect of nuclear charges. The magnitude of the most positive value of V_S, designated as $V_{S,max}$, would indicate and rank the energetically most favored interactive site with the CO_2 molecule. The electrostatic potentials on the surfaces of ScO^+, $Sc_2O_2^+$, and $Sc_3O_4^+$ cations, as well as the position and value of corresponding $V_{S,max}$s are depicted in the bottom panel of Figure 2. The $V_{S,max}$ values, however, show a linear

https://doi.org/10.1021/acs.jpca.4c01562
J. Phys. Chem. A 2024, 128, 3007−3014

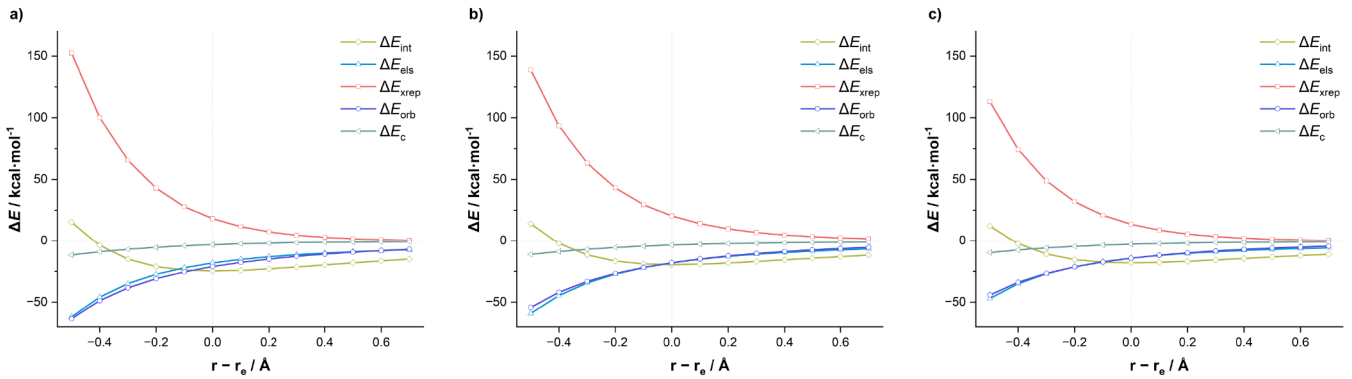

Figure 3. Energy decomposition analysis of the $[ScO(CO_2)]^+$ (a), $[Sc_2O_2(CO_2)]^+$ (b), and $[Sc_3O_4(CO_2)]^+$ (c) ion−molecule complexes projected onto the forming Sc···OCO bond distances *r*. Computations were conducted at the PBE0-D3(BJ)/def2-TZVP level of theory.

relationship with the atomic charge distributions on Sc atoms, implying the limited effectiveness of electrostatic potentials in predicting the binding strengths between cationic scandium oxides and CO_2 molecules.

Apart from the binding strengths, the orientational selectivity of surface−adsorbate interactions are also regarded as a crucial factor for rationalizing the adsorption behaviors in CO_2 heterogeneous catalysis.[3,52,53] Hence, in addition to the varying adsorption capacities of three cationic scandium oxides, the discrepancies in the orientation of the CO_2 molecule relative to each oxide warrant further exploration as well. As illustrated in Figure 2, the $[ScO(CO_2)]^+$ complex ion adopts a bent structure rather than the imaginary linear configuration; while in the $[Sc_2O_2(CO_2)]^+$ complex, the CO_2 molecule resides on top of the $Sc_2O_2^+$ plane with a tilted angle; on the other hand, the $[Sc_3O_4(CO_2)]^+$ complex displays a seemingly less "unusual" coordination mode where the CO_2 molecule is bound in the plane defined by three Sc atoms.

Despite being unable to rigorously reproduce the trend of binding strengths in this case, electrostatic potentials have shown excellent abilities to interpret the site-specific reactivity of molecules from the viewpoint of electrostatic attraction.[54] Accordingly, we turn to pay careful attention to the locations of surface maxima $V_{S,max}$s for the three oxides, which suggest the most feasible sites for interactions with the negative portion of the CO_2 molecules. For the ScO^+ cation, instead of achieving the most positive value at the head region of Sc atom, multiple $V_{S,max}$s with nearly identical values (ca. 12.28 eV) on the side surface are found to surround the Sc atom (see the bottom panel of Figure 2). This circular distribution scenario of electrostatic potentials is in accordance with the optimized binding geometry of the $[ScO(CO_2)]^+$ complex ion. On the contrary, $V_{S,max}$s are located at the head regions of the positively charged Sc atoms of $Sc_2O_2^+$ and $Sc_3O_4^+$ cations. This situation correlates well with the structural arrangement of the $[Sc_3O_4(CO_2)]^+$ complex ion, but the peculiar orientation of CO_2 attached to the $Sc_2O_2^+$ cation has not been recovered. To provide a more intuitive picture of how the electrostatic potential works, the V_S mapped on the respective molecular surfaces of scandium oxide cations and the CO_2 molecule within the framework of optimized complex geometries are displayed in Figure S5. The mismatching overlap between the electron-deficient region on the $Sc_2O_2^+$ cation and the electron-rich area on the CO_2 molecule apparently warrants further discussion.

Overall, neither atomic charge distributions nor molecular electrostatic potentials can correctly predict and rank reaction sites for adsorption of CO_2 on cationic scandium oxides. The inconsistent situation exemplifies a warning against the use of electrostatic arguments as a dictating factor regarding the binding interactions between cationic metal oxides and CO_2 molecules. It is evident that a detailed study is necessary to reconstruct the widely accepted understanding of this binding character.

In attempts to elaborate on the nature of binding interactions between scandium oxide cations and CO_2 molecules, energy decomposition analysis (EDA) was conducted to obtain quantitative descriptions.[55,56] The instantaneous interaction energy (ΔE_{int}) between two fragments (i.e., the cations and CO_2 molecule at the complex geometry) is partitioned into four components with the sobEDA method,[32,41] namely, the electrostatic interaction energy term (ΔE_{els}), the exchange-repulsion energy term (ΔE_{xrep}), the orbital interaction energy term (ΔE_{orb}), and the Coulomb correlation term (ΔE_c) that consists of correlation energy and dispersion correction. Figure 3 presents the results of EDA investigation of the $[ScO(CO_2)]^+$, $[Sc_2O_2(CO_2)]^+$, and $[Sc_3O_4(CO_2)]^+$ complexes along the newly forming Sc···OCO bond distances, with the numerical results calculated at respective equilibrium bond lengths listed in Table 1. The EDA calculations demonstrate that the three complexes share remarkably similar bonding picture. Specifically, the total

Table 1. Energy Decomposition Analysis Results of the Optimized $[ScO(CO_2)]^+$, $[Sc_2O_2(CO_2)]^+$, and $[Sc_3O_4(CO_2)]^+$ Ion−Molecule Complexes at the PBE0-D3(BJ)/def2-TZVP Level of Theory[a]

energy	$[ScO(CO_2)]^+$	$[Sc_2O_2(CO_2)]^+$	$[Sc_3O_4(CO_2)]^+$
ΔE_{int}[b]	−24.70	−19.61	−18.11
ΔE_{xrep}	17.98	20.21	13.49
ΔE_{els}[c]	−18.19 (42.6%)	−18.12 (45.5%)	−14.28 (45.2%)
ΔE_{orb}[c]	−21.13 (49.5%)	−18.02 (45.3%)	−14.36 (45.4%)
ΔE_c[c]	−3.36 (7.9%)	−3.68 (9.2%)	−2.97 (9.4%)

[a]All energy values are given in kcal·mol^{-1}. [b]The absolute value of ΔE_{int} is the expression for the intrinsic bond strength, while binding energies additionally account for the preparation energies required to distort the fragments from the relaxed ground states to the geometries of optimized complexes.[57] [c]The values in parentheses give the percentage contribution to the total attractive interactions ΔE_{els} + ΔE_{orb} + ΔE_c.

https://doi.org/10.1021/acs.jpca.4c01562
J. Phys. Chem. A 2024, 128, 3007−3014

attractive interactions majorly comprise electrostatic and orbital interactions with negligible contribution from correlation terms and are compensated by positive exchange (Pauli) repulsion interactions. A closer inspection of individual attraction terms further reveals an intriguing situation that, instead of being dominated by the electrostatic interactions as expected, the ΔE_{int} is equally stabilized by electrostatic and orbital interactions as indicated by the nearly coinciding ΔE_{els} and ΔE_{orb} curves at all Sc···OCO bond distances shown. Both terms become more stabilizing with decreasing bonding distances, and the orbital interaction in the $[ScO(CO_2)]^+$ complex is even of a higher magnitude than the electrostatic stabilization when the bond begins to form. Consequently, it is conceivable that the bonding situations between cationic scandium oxides and CO_2 molecules cannot be fully explained by solely relying on electrostatic explanations. Orbital interactions, acting as the other main contributor to the attractive terms, must be taken into consideration to comprehensively rationalize the bonding behaviors.

The total electron and orbital deformation density maps upon complexation shown in Figure S6 offer a powerful illustration of the bonding interactions. It clearly indicates the electron density depletion from the C atom and the unbound O atom of the CO_2 molecule as well as the accumulation of electron density in the bonding region. Hence, the bonding patterns between cationic scandium oxide and the CO_2 molecule can be better described as the donor−acceptor interaction, where the positively charged Sc atoms act as Lewis acids accepting electron density from the nucleophilic O atom of CO_2 molecules as Lewis bases. Molecular electrostatic potential is less suitable for predicting such donor−acceptor interactions that involve substantial charge density redistributions as the interacting species approach each other.

Hereby, to clarify the binding strengths and orientational selectivity of CO_2 adsorption on cationic scandium oxides, a surface property on the molecular surface known as the local electron attachment energy, E_S, is introduced to take orbital interactions into account.[58−60] Analogous to the average local ionization energy that is well documented to characterize the susceptibility to electrophilic attacks,[61,62] the E_S has been proven to show the applicability to analyze the propensity for interactions with nucleophiles. The positions where E_S has its lowest value, i.e., the local surface minima $E_{S,min}$, represent the sites prone to accept electron density. Figure 4 displays the graphical visualization of E_S together with the positions and magnitudes of $E_{S,min}$s on the molecular surface of ScO^+, $Sc_2O_2^+$, and $Sc_3O_4^+$ cations. For the ScO^+ cation, the lowest $E_{S,min}$s (−84.21 eV) values are located at nearly the same positions found for the $V_{S,max}$s. The two surface descriptors suggest that the side sites around the Sc atom are the most susceptible to interactions with nucleophiles based on electrostatic and charge transfer arguments, which matches well with the binding orientation of CO_2 in the $[ScO(CO_2)]^+$ complex ion. For the $Sc_2O_2^+$ cation, in contrast to the $V_{S,max}$ which is located along the Sc−Sc bond on the molecular surface, two $E_{S,min}$s were identified to symmetrically reside on either sides of the $Sc_2O_2^+$ plane near the Sc atom with the highest positive charge, which present identical E_S values of −56.62 eV. This result provides an excellent illustration of how the CO_2 molecule orientates itself around Sc atom upon complexation. Specifically, the negatively charged O atom of CO_2 molecule initially approaches the $Sc_2O_2^+$ cation following the guidance of the strongest positive electrostatic potential as

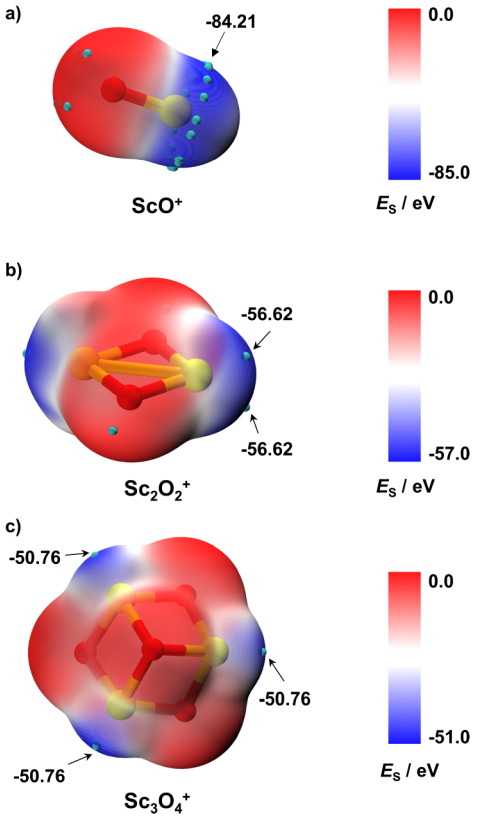

Figure 4. Local electron attachment energy E_S on the molecular surfaces of the ScO^+ (a), $Sc_2O_2^+$ (b), and $Sc_3O_4^+$ (c) cations computed on the 0.004 e/bohr^3 contour of electron density. Cyan dots designate the locations of the corresponding local minima on the surfaces.

indicated by the $V_{S,max}$, then it tilts toward the upper or lower side of the molecular $Sc_2O_2^+$ plane where exhibiting the highest electron accepting tendency as indicated by the two $E_{S,min}$s, and eventually accesses the most favorable bent configuration. The $E_{S,min}$s on the molecular surface of the $Sc_3O_4^+$ cation appear near the head regions of three Sc atoms and coincide with the sites of $V_{S,max}$s, giving a picture of reactive sites consistent with the optimized structure of the $[Sc_3O_4(CO_2)]^+$ complex ion. In addition, the value of $E_{S,min}$s of the $Sc_3O_4^+$ cation (−50.76 eV) is significantly higher than that of the $Sc_2O_2^+$ cation, indicative of a considerably lower nucleophilic reactivity than that of $Sc_2O_2^+$. The exceptional agreements between the binding strengths in terms of CO_2 adsorption on cationic scandium oxides and the magnitudes of the $E_{S,min}$s on the corresponding oxide surfaces, in conjunction with the binding orientations and the positions of the $E_{S,min}$s, highlight the pivotal role of orbital interactions in governing the CO_2 binding abilities and motifs of positively charged scandium oxides.

The decreasing adsorption capabilities along the series of ScO^+ > $Sc_2O_2^+$ > $Sc_3O_4^+$ cation prompt us to reflect on the correlation between the E_S and the different reactivity patterns over the inequivalent surface of bulk materials. The major difference among the chemical environments of Sc atoms in the three oxides is the coordination number (CN) of the metal atoms, which varies from CN = 1 in ScO^+ to 3 in the $Sc_3O_4^+$ cation. The increasing degree of the coordinative saturation of the metal atoms leads to the weakened capability to accept electron transfer from donor molecules, as represented by the

https://doi.org/10.1021/acs.jpca.4c01562
J. Phys. Chem. A 2024, 128, 3007−3014

reduced absolute values of $E_{S,min}$s on the corresponding oxide surfaces. When it comes to real catalytic systems, the CO_2 adsorption behaviors of heterogeneous metal oxide catalysts are significantly affected by the structural defects present on the surfaces. Coordinatively unsaturated sites where the local minima $E_{S,min}$s are expected to be situated, such as metal centers adjacent to oxygen vacancies and those located at corner and edge sites, have been observed to enhance the binding of CO_2 molecules to the surface.[63−65] Hence, the surface property E_S can be applied as a complementary way to predict coordination sites susceptible to electron-donating molecules and assess relative interaction tendencies for different sites over transition metal oxide surfaces.

It should be emphasized that the electrostatic potential V_S identifies both sites susceptible to electrophilic and nucleophilic attacks from the long-range electrostatic attraction perspective, whereas the local electron attachment energy E_S can be used only to characterize the site-resolved susceptibilities for nucleophilic attacks based on short-range orbital interactions. Therefore, the combination of these two theoretical descriptors can provide a complete reactivity picture in surface−adsorbate systems composed of transition metal oxides and nucleophilic molecules.

4. CONCLUSIONS

In summary, we characterized the binding configuration of the $Sc_3O_4^+$ cation and the CO_2 molecule using integrated infrared photodissociation spectroscopy and theoretical study. By comparison with the $[ScO(CO_2)]^+$ and $[Sc_2O_2(CO_2)]^+$ ion−molecule complexes, a decreasing trend in the interaction strengths and notable variations in binding orientations between cationic scandium oxides and CO_2 molecules were noticed. NPA atomic charges and electrostatic potentials on the molecular surfaces were first employed to analyze the propensity of cationic scandium oxides for CO_2 adsorption based on widely accepted electrostatic considerations. However, no strict correlation between electrostatic interactions and the binding strengths as well as preferred orientations has been established due to the discrepant results, which raises the question of whether the electrostatic attractions dominate the adsorption behaviors of cationic scandium oxides upon exposure to CO_2 molecules. Quantitative EDA calculations reveal the critical role of orbital interactions in governing the binding processes during the adsorption of CO_2 on cationic scandium oxides. The local electron attachment energy was introduced thereby to account for orbital interactions, which satisfactorily rationalized the affinities and orientational preferences of cationic scandium oxides toward interactions with CO_2 molecules. Overall, the combination of two surface properties, including electrostatic potential and local electron attachment energy, is expected to be an effective tool for predicting and analyzing orientational selectivity and quantitatively ranking local surface affinities for the adsorption of CO_2 on transition metal oxide surfaces.

■ ASSOCIATED CONTENT

Supporting Information

The Supporting Information is available free of charge at https://pubs.acs.org/doi/10.1021/acs.jpca.4c01562.

Typical TOF mass spectrum produced by pulsed laser vaporization of a scandium metal target in expansion of helium seeded with carbon dioxide (Figure S1); low-lying, PBE0-D3(BJ)/def2-TZVP optimized isomer structures of $Sc_3O_4^+$ cation in the singlet state with their relative zero-point corrected energies (Figure S2); low-lying, PBE0-D3(BJ)/def2-TZVP optimized isomers of the $[Sc_3O_4(CO_2)]^+$ ion−molecule complex with their relative zero-point corrected energies (Figure S3); possible explanations for the low-frequency band in the experimental spectrum of the $[Sc_3O_4(CO_2)]^+$ complex ion (Figure S4); electrostatic potentials on the respective molecular surfaces of the ScO^+, $Sc_2O_2^+$ and $Sc_3O_4^+$ cations and CO_2 molecule computed on the 0.001 e/bohr^3 contour of electron density (Figure S5); electron and orbital deformation density maps of the complexation processes for the $[ScO(CO_2)]^+$, $[Sc_2O_2(CO_2)]^+$, and $[Sc_3O_4(CO_2)]^+$ ion−molecule complexes (Figure S6) (PDF)

■ AUTHOR INFORMATION

Corresponding Authors

Jia Han − *Hefei National Research Center for Physical Sciences at the Microscale, University of Science and Technology of China, Hefei 230026, China*; Email: jiahan@ustc.edu.cn

Xiaoguo Zhou − *Hefei National Research Center for Physical Sciences at the Microscale and Department of Chemical Physics, University of Science and Technology of China, Hefei 230026, China*; orcid.org/0000-0002-0264-0146; Email: xzhou@ustc.edu.cn

Weijun Zhang − *Anhui Institute of Optics and Fine Mechanics, Hefei Institutes of Physical Science, Chinese Academy of Sciences, Hefei 230031, China*; Email: wjzhang@aiofm.ac.cn

Authors

Pengcheng Liu − *Anhui Institute of Optics and Fine Mechanics, Hefei Institutes of Physical Science, Chinese Academy of Sciences, Hefei 230031, China; Science Island Branch, Graduate School, University of Science and Technology of China, Hefei 230026, China*

Yan Chen − *Department of Chemical Physics, University of Science and Technology of China, Hefei 230026, China*

Haili Yu − *Department of Chemical Physics, University of Science and Technology of China, Hefei 230026, China*

Complete contact information is available at: https://pubs.acs.org/10.1021/acs.jpca.4c01562

Notes

The authors declare no competing financial interest.

■ ACKNOWLEDGMENTS

This work was financially supported by the National Natural Science Foundation of China (nos. 22073088, 91544228 and 21903079). X.Z. is also grateful for the support of the Fundamental Research Funds for the Central Universities. All DFT calculations were performed on the supercomputing system in the Supercomputing Center of the University of Science and Technology of China.

■ REFERENCES

(1) Fennell, P. S.; Shah, N.; Maitland, G. C. The Role of CO_2 Capture and Utilization in Mitigating Climate Change. *Nat. Clim. Change* **2017**, *7*, 243−249.

(2) Gao, W.; Liang, S.; Wang, R.; Jiang, Q.; Zhang, Y.; Zheng, Q.; Xie, B.; Toe, C. Y.; Zhu, X.; Wang, J.; et al.et al. Industrial Carbon

Dioxide Capture and Utilization: State of the Art and Future Challenges. *Chem. Soc. Rev.* **2020**, *49*, 8584−8686.
(3) Baltrusaitis, J.; Schuttlefield, J.; Zeitler, E.; Grassian, V. H. Carbon Dioxide Adsorption on Oxide Nanoparticle Surfaces. *Chem. Eng. J.* **2011**, *170*, 471−481.
(4) Taifan, W.; Boily, J.-F.; Baltrusaitis, J. Surface Chemistry of Carbon Dioxide Revisited. *Surf. Sci. Rep.* **2016**, *71*, 595−671.
(5) Tayyebi, E.; Hussain, J.; Abghoui, Y.; Skúlason, E. Trends of Electrochemical CO_2 Reduction Reaction on Transition Metal Oxide Catalysts. *J. Phys. Chem. C* **2018**, *122*, 10078−10087.
(6) Omodolor, I. S.; Otor, H. O.; Andonegui, J. A.; Allen, B. J.; Alba-Rubio, A. C. Dual-Function Materials for CO_2 Capture and Conversion: A Review. *Ind. Eng. Chem. Res.* **2020**, *59*, 17612−17631.
(7) Burghaus, U. Surface chemistry of CO_2 − Adsorption of Carbon Dioxide on Clean Surfaces at Ultrahigh Vacuum. *Prog. Surf. Sci.* **2014**, *89*, 161−217.
(8) Weber, J. M. The Interaction of Negative Charge with Carbon Dioxide − Insight into Solvation, Speciation and Reductive Activation from Cluster Studies. *Int. Rev. Phys. Chem.* **2014**, *33*, 489−519.
(9) Schwarz, H.; Asmis, K. R. Identification of Active Sites and Structural Characterization of Reactive Ionic Intermediates by Cryogenic Ion Trap Vibrational Spectroscopy. *Chem. - Eur. J.* **2019**, *25*, 2112−2126.
(10) Knurr, B. J.; Weber, J. M. Structures of $[CoO(CO_2)_n]^-$ and $[NiO(CO_2)n]^-$ Clusters Studied by Infrared Spectroscopy. *J. Phys. Chem. A* **2015**, *119*, 843−850.
(11) Dodson, L. G.; Thompson, M. C.; Weber, J. M. Interactions of Molecular Titanium Oxides TiO_x (x = 1−3) with Carbon Dioxide in Cluster Anions. *J. Phys. Chem. A* **2018**, *122*, 6909−6917.
(12) Debnath, S.; Song, X.; Fagiani, M. R.; Weichman, M. L.; Gao, M.; Maeda, S.; Taketsugu, T.; Schöllkopf, W.; Lyalin, A.; Neumark, D. M.; et al.et al. CO_2 Adsorption on $Ti_3O_6^-$: A Novel Carbonate Binding Motif. *J. Phys. Chem. C* **2019**, *123*, 8439−8446.
(13) Zhou, M.; Zhou, Z.; Zhuang, J.; Li, Z. H.; Fan, K.; Zhao, Y.; Zheng, X. Carbon Dioxide Coordination and Activation by Niobium Oxide Molecules. *J. Phys. Chem. A* **2011**, *115*, 14361−14369.
(14) Zhuang, J.; Li, Z. H.; Fan, K.; Zhou, M. Matrix Isolation Spectroscopic and Theoretical Study of Carbon Dioxide Activation by Titanium Oxide Molecules. *J. Phys. Chem. A* **2012**, *116*, 3388−3395.
(15) Flores, L. A.; Murphy, J. G.; Copeland, W. B.; Dixon, D. A. Reaction of CO_2 with Groups 4 and 6 Transition Metal Oxide Clusters. *J. Phys. Chem. A* **2017**, *121*, 8719−8727.
(16) Zhao, Z.; Kong, X.; Yuan, Q.; Xie, H.; Yang, D.; Zhao, J.; Fan, H.; Jiang, L. Coordination-Induced CO_2 Fixation into Carbonate by Metal Oxides. *Phys. Chem. Chem. Phys.* **2018**, *20*, 19314−19320.
(17) Iskra, A.; Gentleman, A. S.; Cunningham, E. M.; Mackenzie, S. R. Carbon Dioxide Binding to Metal Oxides: Infrared Spectroscopy of $NbO_2^+(CO_2)_n$ and $TaO_2^+(CO_2)_n$ Complexes. *Int. J. Mass Spectrom.* **2019**, *435*, 93−100.
(18) Yang, D.; Su, M.-Z.; Zheng, H.-J.; Zhao, Z.; Kong, X.-T.; Li, G.; Xie, H.; Zhang, W.-Q.; Fan, H.-J.; Jiang, L. Infrared Spectroscopy of CO_2 Transformation by Group III Metal Monoxide Cations. *Chin. J. Chem. Phys.* **2020**, *33*, 160−166.
(19) Brewer, E. I.; Green, A. E.; Gentleman, A. S.; Beardsmore, P. W.; Pearcy, P. A. J.; Meizyte, G.; Pickering, J.; Mackenzie, S. R. An Infrared Study of CO_2 Activation by Holmium Ions, Ho^+ and HoO^+. *Phys. Chem. Chem. Phys.* **2022**, *24*, 22716−22723.
(20) Liu, P.; Han, J.; Chen, Y.; Lu, S.; Su, Q.; Zhou, X.; Zhang, W. Carbon Dioxide Activation by Discandium Dioxide Cations in the Gas Phase: A Combined Investigation of Infrared Photodissociation Spectroscopy and DFT Calculations. *Phys. Chem. Chem. Phys.* **2023**, *25*, 32853−32862.
(21) Phoung, S.; Williams, E.; Gaustad, G.; Gupta, A. Exploring Global Supply and Demand of Scandium Oxide in 2030. *J. Cleaner Prod.* **2023**, *401*, 136673.
(22) Deng, G.; Li, C.-J. $Sc(OTf)_3$-Catalyzed Direct Alkylation of Quinolines and Pyridines with Alkanes. *Org. Lett.* **2009**, *11*, 1171−1174.
(23) Wu, X.-N.; Xu, B.; Meng, J.-H.; He, S.-G. C−H Bond Activation by Nanosized Scandium Oxide Clusters in Gas-Phase. *Int. J. Mass Spectrom.* **2012**, *310*, 57−64.
(24) Hwang, D.-Y.; Mebel, A. M. Activation of Methane by Neutral Transition Metal Oxides (ScO, NiO, and PdO): A Theoretical Study. *J. Phys. Chem. A* **2002**, *106*, 12072−12083.
(25) Pu, Y.-C.; Li, S.-R.; Yan, S.; Huang, X.; Wang, D.; Ye, Y.-Y.; Liu, Y.-Q. An Improved Cu/ZnO Catalyst Promoted by Sc_2O_3 for Hydrogen Production from Methanol Reforming. *Fuel* **2019**, *241*, 607−615.
(26) Chen, Y.; Xin, K.; Jin, J.; Li, W.; Wang, Q.; Wang, X.; Wang, G. Infrared Photodissociation Spectroscopic Investigation of $TMO(CO)_n^+$ (TM = Sc, Y, La): Testing the 18-Electron Rule. *Phys. Chem. Chem. Phys.* **2019**, *21*, 6743−6749.
(27) Chen, Y.; Jin, J.; Xin, K.; Yu, W.; Xing, X.; Wang, X.; Wang, G. Infrared Photodissociation Spectroscopic Studies of $ScO(H_2O)_{n=1-3}Ar^+$ Cluster Cations: Solvation Induced Reaction of ScO^+ and Water. *Phys. Chem. Chem. Phys.* **2019**, *21*, 15639−15646.
(28) Liu, Z.; Hou, L.; Li, Y.; Li, G.; Qin, Z.; Wu, H.-S.; Jia, J.; Xie, H.; Tang, Z. Thermodynamics and Kinetics of Gas-Phase CO Oxidation on the Scandium Monoxide Carbonyl Complexes. *J. Phys. Chem. A* **2020**, *124*, 924−931.
(29) Cui, J.; Zhao, Y.; Wang, M.; Wang, S.; Ma, J. Thermal Benzene Activation by 3d Transition Metal (Sc-Cu) Oxide Cations. *Chin. Chem. Lett.* **2020**, *31*, 779−782.
(30) Zhao, Y.-X.; Yuan, J.-Y.; Ding, X.-L.; He, S.-G.; Zheng, W.-J. Electronic Structure and Reactivity of a Biradical Cluster: $Sc_3O_6^-$. *Phys. Chem. Chem. Phys.* **2011**, *13*, 10084−10090.
(31) Mansley, Z. R.; Mizzi, C. A.; Koirala, P.; Wen, J.; Marks, L. D. Structure of the (110) $LnScO_3$ (Ln = Gd, Tb, Dy) Surfaces. *Phys. Rev. Mater.* **2020**, *4*, 045003.
(32) Lu, T.; Chen, F. Multiwfn: A Multifunctional Wavefunction Analyzer. *J. Comput. Chem.* **2012**, *33*, 580−592.
(33) Lu, T.. *Molclus Program*. http://www.keinsci.com/research/molclus.html, 2023.
(34) Bannwarth, C.; Ehlert, S.; Grimme, S. GFN2-xTB—An Accurate and Broadly Parametrized Self-Consistent Tight-Binding Quantum Chemical Method with Multipole Electrostatics and Density-Dependent Dispersion Contributions. *J. Chem. Theory Comput.* **2019**, *15*, 1652−1671.
(35) Grimme, S.; Bannwarth, C.; Shushkov, P. A Robust and Accurate Tight-Binding Quantum Chemical Method for Structures, Vibrational Frequencies, and Noncovalent Interactions of Large Molecular Systems Parametrized for All spd-Block Elements (Z = 1−86). *J. Chem. Theory Comput.* **2017**, *13*, 1989−2009.
(36) Adamo, C.; Barone, V. Toward Reliable Density Functional Methods without Adjustable Parameters: The PBE0Model. *J. Chem. Phys.* **1999**, *110*, 6158−6170.
(37) Grimme, S.; Ehrlich, S.; Goerigk, L. Effect of the Damping Function in Dispersion Corrected Density Functional Theory. *J. Comput. Chem.* **2011**, *32*, 1456−1465.
(38) Frisch, M. J.; Trucks, G. W.; Schlegel, H. B.; Scuseria, G. E.; Robb, M. A.; Cheeseman, J. R.; Scalmani, G.; Barone, V.; Petersson, G. A.; Nakatsuji, H., et al.et al. Gaussian 16 Rev. C.01; Gaussian, Inc.: Wallingford, CT, 2016.
(39) Raghavachari, K.; Trucks, G. W.; Pople, J. A.; Head-Gordon, M. A Fifth-Order Perturbation Comparison of Electron Correlation Theories. *Chem. Phys. Lett.* **1989**, *157*, 479−483.
(40) Neese, F. The ORCA Program System. *Wiley Interdiscip. Rev.: Comput. Mol. Sci.* **2012**, *2*, 73−78.
(41) Lu, T.; Chen, Q. Simple, Efficient, and Universal Energy Decomposition Analysis Method Based on Dispersion-Corrected Density Functional Theory. *J. Phys. Chem. A* **2023**, *127*, 7023−7035.
(42) Yang, Y.; Liu, H.; Zhang, P. Structural and Electronic Properties of Sc_nO_m (n = 1−3, m = 1−2n) Clusters: Theoretical Study Using Screened Hybrid Density Functional Theory. *Phys. Rev. B* **2011**, *84*, 205430.

https://doi.org/10.1021/acs.jpca.4c01562
J. Phys. Chem. A 2024, 128, 3007−3014

(43) Wu, L.; Zhang, C.; Krasnokutski, S. A.; Yang, D.-S. Mass-Analyzed Threshold Ionization and Structural Isomers of M_3O_4 (M = Sc, Y, and La). *J. Chem. Phys.* **2012**, *137* (8), 084312.
(44) Sodupe, M.; Branchadell, V.; Rosi, M.; Bauschlicher, C. W. Theoretical Study of M^+-CO_2 and OM^+CO Systems for First Transition Row Metal Atoms. *J. Phys. Chem. A* **1997**, *101*, 7854−7859.
(45) Duncan, M. A. Infrared Spectroscopy to Probe Structure and Dynamics in Metal Ion−Molecule Complexes. *Int. Rev. Phys. Chem.* **2003**, *22*, 407−435.
(46) Zimmermann, N.; Bernhardt, T. M.; Bakker, J. M.; Barnett, R. N.; Landman, U.; Lang, S. M. Infrared Spectroscopy of Gas-Phase $Mn_xO_y(CO_2)_z^+$ Complexes. *J. Phys. Chem. A* **2020**, *124*, 1561−1566.
(47) Kong, X.; Shi, R.; Wang, C.; Zheng, H.; Wang, T.; Liang, X.; Yang, J.; Jing, Q.; Liu, Y.; Han, H.; et al.et al. Interaction between CO_2 and NbO_2^+: Infrared Photodissociation Spectroscopic and Theoretical Study. *Chem. Phys.* **2020**, *534*, 110755.
(48) Walker, N. R.; Grieves, G. A.; Walters, R. S.; Duncan, M. A. The Metal Coordination in $Ni^+(CO_2)$n and $NiO_2^+(CO_2)_m$ Complexes. *Chem. Phys. Lett.* **2003**, *380*, 230−236.
(49) Politzer, P.; Murray, J. S. The Fundamental Nature and Role of the Electrostatic Potential in Atoms and Molecules. *Theor. Chem. Acc.* **2002**, *108*, 134−142.
(50) Murray, J. S.; Politzer, P. The Electrostatic Potential: An Overview. *WIREs Comput. Mol. Sci.* **2011**, *1*, 153−163.
(51) Murray, J. S.; Politzer, P. Molecular Electrostatic Potentials and Noncovalent Interactions. *WIREs Comput. Mol. Sci.* **2017**, *7* (6), No. e1326.
(52) Mino, L.; Spoto, G.; Ferrari, A. M. CO_2 Capture by TiO_2 Anatase Surfaces: A Combined DFT and FTIR Study. *J. Phys. Chem. C* **2014**, *118*, 25016−25026.
(53) Chen, H.-Y. T.; Tosoni, S.; Pacchioni, G. A DFT Study of the Acid−Base Properties of Anatase TiO_2 and Tetragonal ZrO_2 by Adsorption of CO and CO_2 Probe Molecules. *Surf. Sci.* **2016**, *652*, 163−171.
(54) Grimmel, S. A.; Reiher, M. The Electrostatic Potential as A Descriptor for the Protonation Propensity in Automated Exploration of Reaction Mechanisms. *Faraday Discuss.* **2019**, *220*, 443−463.
(55) Hopffgarten, M. V.; Frenking, G. Energy Decomposition Analysis. *WIREs Comput. Mol. Sci.* **2012**, *2*, 43−62.
(56) Zhao, L.; von Hopffgarten, M.; Andrada, D. M.; Frenking, G. Energy Decomposition Analysis. *WIREs Comput. Mol. Sci.* **2018**, *8* (3), No. e1345.
(57) Zhao, L.; Hermann, M.; Schwarz, W. H. E.; Frenking, G. The Lewis Electron-Pair Bonding Model: Modern Energy Decomposition Analysis. *Nat. Rev. Chem.* **2019**, *3*, 48−63.
(58) Brinck, T.; Carlqvist, P.; Stenlid, J. H. Local Electron Attachment Energy and Its Use for Predicting Nucleophilic Reactions and Halogen Bonding. *J. Phys. Chem. A* **2016**, *120*, 10023−10032.
(59) Stenlid, J. H.; Brinck, T. Nucleophilic Aromatic Substitution Reactions Described by the Local Electron Attachment Energy. *J. Org. Chem.* **2017**, *82*, 3072−3083.
(60) Halldin Stenlid, J.; Johansson, A. J.; Brinck, T. The Local Electron Attachment Energy and the Electrostatic Potential as Descriptors of Surface−Adsorbate Interactions. *Phys. Chem. Chem. Phys.* **2019**, *21*, 17001−17009.
(61) Bulat, F. A.; Murray, J. S.; Politzer, P. Identifying the Most Energetic Electrons in a Molecule: The Highest Occupied Molecular Orbital and the Average Local Ionization Energy. *Comput. Theor. Chem.* **2021**, *1199*, 113192.
(62) Han, J.; Wang, L.; Cao, W.; Yuan, Q.; Zhou, X.; Liu, S.; Wang, X.-B. Manifesting Direction-Specific Complexation in $[HFIP_{-H}\cdot H_2O_2]^-$: Exclusive Formation of a High-Lying Conformation. *J. Phys. Chem. Lett.* **2022**, *13*, 8607−8612.
(63) Jiang, W.; Loh, H.; Low, B. Q. L.; Zhu, H.; Low, J.; Heng, J. Z. X.; Tang, K. Y.; Li, Z.; Loh, X. J.; Ye, E.; et al.et al. Role of Oxygen Vacancy in Metal Oxides for Photocatalytic CO_2 Reduction. *Appl. Catal., B* **2023**, *321*, 122079.
(64) Jia, J.; Qian, C.; Dong, Y.; Li, Y. F.; Wang, H.; Ghoussoub, M.; Butler, K. T.; Walsh, A.; Ozin, G. A. Heterogeneous Catalytic Hydrogenation of CO_2 by Metal Oxides: Defect Engineering − Perfecting Imperfection. *Chem. Soc. Rev.* **2017**, *46*, 4631−4644.
(65) Behrens, M.; Studt, F.; Kasatkin, I.; Kühl, S.; Hävecker, M.; Abild-Pedersen, F.; Zander, S.; Girgsdies, F.; Kurr, P.; Kniep, B.-L.; et al.et al. The Active Site of Methanol Synthesis over $Cu/ZnO/Al_2O_3$ Industrial Catalysts. *Science* **2012**, *336*, 893−897.

https://doi.org/10.1021/acs.jpca.4c01562
J. Phys. Chem. A 2024, 128, 3007−3014